A study of the magnetic transitions in CuO: specific heat (1-330 K), magnetic susceptibility and phonon density of states

1989 J. Phys.: Condens. Matter 1 8021

(http://iopscience.iop.org/0953-8984/1/43/004)

J. Phys.: Condens. Matter 1 (1989) 8021–8034. Printed in the UK

A study of the magnetic transitions in CuO: specific heat (1–330 K), magnetic susceptibility and phonon density of states

A Junod†, D Eckert†, G Triscone†, J Müller† and W Reichardt‡

† Département de physique de la matière condensée, Université de Genève, CH-1211 Genève 4, Switzerland

‡ Kernforschungszentrum Karlsruhe, Institut für Nukleare Festkörperphysik, PO Box 3640, D7500 Karlsruhe, Federal Republic of Germany and Laboratoire Léon Brillouin, Laboratoire commun CEA-CNRS, CEN Saclay, F-91191 Gif-sur-Yvette, France

Received 24 January 1989, in final form 31 March 1989

Abstract. The specific heat C_p (1–330 K) and magnetic susceptibility χ (5–250 K) of a CuO sample sintered and annealed in oxygen are presented. In contrast with some earlier results, we find:

(i) an essentially zero linear term in the low-temperature specific heat ($\gamma^* < 0.05$ mJ mol^{-1} K^{-2});

(ii) a minor change in slope in the susceptibility curve and a critical point in C_p at the antiferromagnetic transition ($T_N = 229.5 \pm 0.5$ K);

(iii) a first-order peak in C_p at the commensurate–incommensurate transition ($T_M = 212.6 \pm 0.5$ K, $\Delta H = 4.5 \pm 0.3$ J mol^{-1});

(iv) a smooth variation of the susceptibility below T_M.

The phonon density-of-states is determined by inelastic neutron scattering on a single crystal at room temperature, thus enabling a separation of the lattice and magnetic contributions to C_p. A large contribution due to short-range order is observed above T_N, and it is concluded that CuO behaves as a 1D or 2D Heisenberg antiferromagnet.

Thermodynamic functions are tabulated up to room temperature.

1. Introduction

Recent developments in high-temperature superconductivity have focused interest on oxides containing square-planar coordinated Cu^{2+} ions. Their magnetic properties are unusual. Superconductivity in copper-based ceramics apparently always occurs on the verge of frustrated low-dimensional antiferromagnetic order in Cu–O planes or chains. Cupric oxide, or natural tenorite, has a structure of interleaved CuO_2 sheets with square-planar coordination of copper by oxygen [1], unlike the other 3d transition-element monoxides which have octahedral coordination. Early work on CuO indicated an anomalous magnetic behaviour. Antiferromagnetic ordering at $T_N = 230$ K ($\mu_{eff} = 0.6 \pm 0.1\ \mu_B$) was found by neutron diffraction on powder [2], but neither a Curie–Weiss behaviour nor a cusp at T_N was found in the magnetic susceptibility; instead, a broad maximum near 600 K and a break in the slope at 130 K were observed [3, 4]. A change of slope in the vicinity of 230 K was reported in more recent work [5, 6]. A smeared step

0953-8984/89/438021 + 14 $02.50

was detected in the specific heat near 220 K [7]; its amplitude (see figure 4 later) was considerably smaller than for MnO [8], FeO [8], CoO [9] and NiO [10], the order of magnitude being 10–20 J mol^{-1} K^{-1} in the latter cases.

Further characterisation was obtained recently. Diffraction work on a single crystal [11] disclosed a double magnetic transition: an incommensurate antiferromagnetic structure forms below the Néel temperature at 230 ± 1 K, and the propagation vector becomes commensurate with the lattice at 213 ± 1 K; it stays so down to 20 K at least. Loram and co-workers [12], hereafter referred to as LMJO, resolved a two-peak structure at 212 and 230 K by high-resolution calorimetry, and evaluated the magnetic entropy by subtracting the extrapolated lattice specific heat. From this and from a fit of the existing susceptibility data, they concluded that CuO behaves as a 1D antiferromagnet showing short-range magnetic order above T_N. They remarked that the presence of these correlations may be reconciled with the absence of paramagnetic scattering above T_N [11] if fluctuations occur on a short time scale ($\ll 10^{-7}$ s).

Using a different high-resolution calorimetric technique, we present here results obtained with a polycrystalline sample that has been carefully oxidised. Sharp calorimetric transitions at 212.6(5) K and 229.5(5) K are characterised. Furthermore, we are in a position to subtract the lattice specific heat using the phonon density-of-states (DOS) measured by neutron scattering, thus gaining access to the magnetic contribution over most of the temperature range without additional hypotheses (except for a small correction C_p–C_V). Magnetic susceptibility data are presented, in particular near the Néel point and in the 130–140 K region.

2. Sample preparation and characterisation

Sample A was prepared from >99% pure CuO powder supplied by Fluka AG, pelletised at ≈5 tons cm^{-2} without any further treatment. Only low temperature (<15 K) specific heat measurements were performed on this first sample, which supposedly contains oxygen vacancies. The results appeared in [13] along with other phases in the Y–Ba–Cu–O system.

The same starting material was used for sample B, but the heat treatment was inspired by the preparation of $YBa_2Cu_3O_7$ superconducting samples, which are known to be most sensitive to oxygen stoichiometry. The pressed powder was sintered under flowing oxygen at 950 °C during 12 hours, and then cooled in oxygen down to room temperature at the rate of −70 °C h^{-1}. The purpose of this treatment was to suppress oxygen vacancies, and to eliminate the possibility of hydrated oxide formation. The resulting material was dark grey and slightly shiny. The disk shape (diameter ≈10 mm, thickness ≈0.8 mm) was optimised for a good heat transfer in specific heat (C_p) measurements. The whole sample (0.28 g) was used for the C_p measurements above 30 K. It was broken down into smaller pieces for low-temperature calorimetry, susceptibility and x-ray measurements.

No impurity lines were found in x-ray Guinier patterns. The parameters of the monoclinic cell, calibrated with a Si standard, are a = 4.6887(9) Å, b = 3.4248(8) Å, c = 5.1321(8) Å, and β = 99.55(2)°; V = 81.27 $Å^3$. This is comparable, but systematically higher than the refinement of [14] who find a = 4.6837(5) Å, b = 3.4226(5) Å, c = 5.1288(6) Å, and β = 99.54(1)°; V = 81.08 $Å^3$. Earlier data by Tunnell and co-workers, [1] show much smaller parameters (a = 4.662 Å, b = 3.417 Å, c = 5.118 Å, β = 97.48°, V = 80.84 $Å^3$). These variations may be taken as an indication of oxygen non-stoichiometry. The average grain size according to microstructural examinations is 50–100 μm. Twinning of all grains is made apparent by using polarised light.

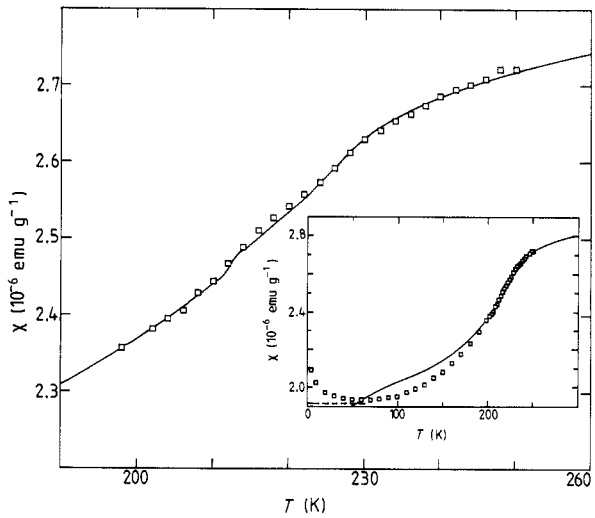

Figure 1. Susceptibility of CuO in the region of the magnetic transitions. Squares, experimental data; full curve, calculated curve according to Fisher's relation (see text). Inset: same data over the full temperature range; broken line, initial susceptibility after correction for an extrinsic Curie term.

The resistance of the sample exceeds 10 MΩ at 77 K.

3. Experimental procedure

A SQUID magnetometer was used for magnetic susceptibility measurements from 5 to 250 K [15]. A correction for saturable moments using 0.5 and 2 T data was applied. These impurity moments are equivalent to 5.6 ppm by weight of ferromagnetic iron. The corrected data reported here were then taken at 0.5 T.

The low-temperature specific heat measurements (1.3–20 K) were performed with a microcomputer-controlled thermal relaxation method, on samples weighing 90 mg. The heat capacity of the addenda (sample holder, thermometer) was measured separately and subtracted. The uncertainty on the results is estimated to be less than 5%.

From 30 to 300 K we used a computerised version of the adiabatic, constant heating method [16]. The measurement was done with increasing temperatures at an average rate of 8–10 mK s^{-1}. Platinum thermometry was used. The heat capacity of the addenda contributed to about one-half of the total. It was measured separately with a reproducibility of ±0.3% and subtracted. The accuracy has recently been reassessed. The specific heat of a 99.999% pure copper sample (mass 0.8 g) did not deviate from reference data [17] by more than ±1%. The agreement between the present data on CuO and the earlier work by Hu and Johnston [7], who used a 162 g sample (2 mol), is of the order of 1% outside of the transition region (see figure 4 later). Close to the magnetic transitions, the present data show a more detailed structure owing to the improved resolution and better sample homogeneity.

4. Results

4.1. Magnetic susceptibility

The susceptibility measurements for sample B are presented in figure 1. The antiferromagnetic transition near $T_N = 230$ K is barely visible as a change in the slope. The shape and smallness of the anomaly are unusual (see e.g. [18] for a review), but will be

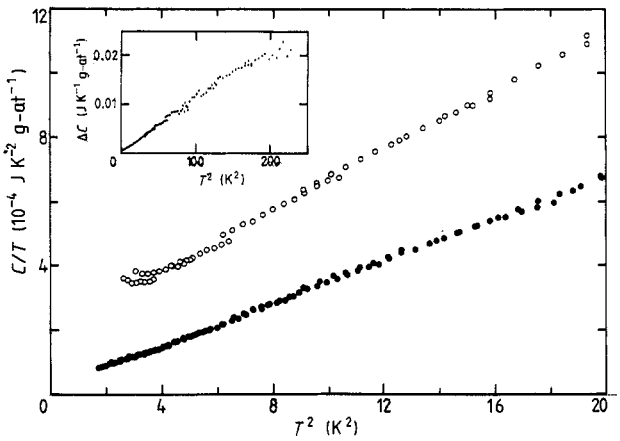

Figure 2. Specific heat of CuO below 4.5 K divided by the temperature versus temperature squared. Open circles, pressed powder sample; full circles, sample sintered in oxygen. Inset: difference between the specific heats of the above samples plotted versus T^2. 1 mole = 2 gram-atom = 79.55 g.

shown to be consistent with thermal data. It may be worth recalling that a ferromagnetic transition is suppressed by an homogeneous magnetic field, but an antiferromagnetic transition is *not*. Below 210 K, the curvature of the susceptibility data is smooth and, at variance with earlier measurements [3], does not suggest any anomaly near 140 K. The sample-dependent rise below 50 K [19, 3] appears to be due to localised moments of extrinsic origin.

An AC susceptibility measurement in 0.1 G RMS did not reveal any anomaly in the 200–240 K range.

4.2. Low-temperature specific heat

The low-temperature specific heat data for samples A and B are presented in figure 2. Internal time constants ('τ_2 effects') prevented meaningful data collection below 2 K in the pressed-powder sample A; this problem disappeared in the sintered sample B.

We first concentrate on the low-temperature specific heat of sample B. The ratio C/T does not extrapolate exactly to zero at $T \rightarrow 0$, indicating the presence of non-phonon terms. Polynomial fits in the temperature range 1–20 K did not determine unambiguously the form of these extra terms. The lattice specific heat was represented by $C_l = \beta T^3 + \delta T^5$. The other terms tested were $C = AT^{-2}$ (Schottky tail), $C = \gamma^* T$ (two-level systems [20] or 1D antiferromagnetic spin waves), $C = BT^2$ (surface phonons or 2D antiferromagnetic spin waves), or combinations thereof. The lowest residuals using a single non-phonon term were obtained with $\gamma^* \simeq 22\ \mu\text{J K}^{-2}\ \text{g-at}^{-1}$ and $\theta(0) = 392$ K; using simultaneously two non-phonon terms, a combination of T^{-2} and T^2 terms was preferred. From these and other fits, we obtain conservative estimates: $\theta(0) = 390 \pm 10$ K, $\gamma^* < 25\ \mu\text{J K}^{-2}\ \text{g-at}^{-1}$, $A < 75\ \mu\text{J K g-at}^{-1}$ and $\delta \simeq -0.01\ \mu\text{J K}^{-6}\ \text{g-at}^{-1}$.

At first glance, the initial Debye temperature for sample A seems to be lower and γ^* higher (figure 2, curve A). In fact, the *difference* between both curves is proportional to T^2 within experimental scatter (figure 2, inset) from 2 K to the upper limit of the measurement for sample A. This gives strong support to a contribution of surface phonons in the pressed-powder material. Similar effects have been reported, e.g. in Al_2O_3 [21]. In a limited temperature interval such as that of figure 2, a single T^2 term is indistinguishable from a superposition of linear and cubic terms, and apparent γ^*s attributed to localised surface states in the energy gap [12] or to two-level systems [20] may be due to phonon surface modes in imperfectly crystallised material.

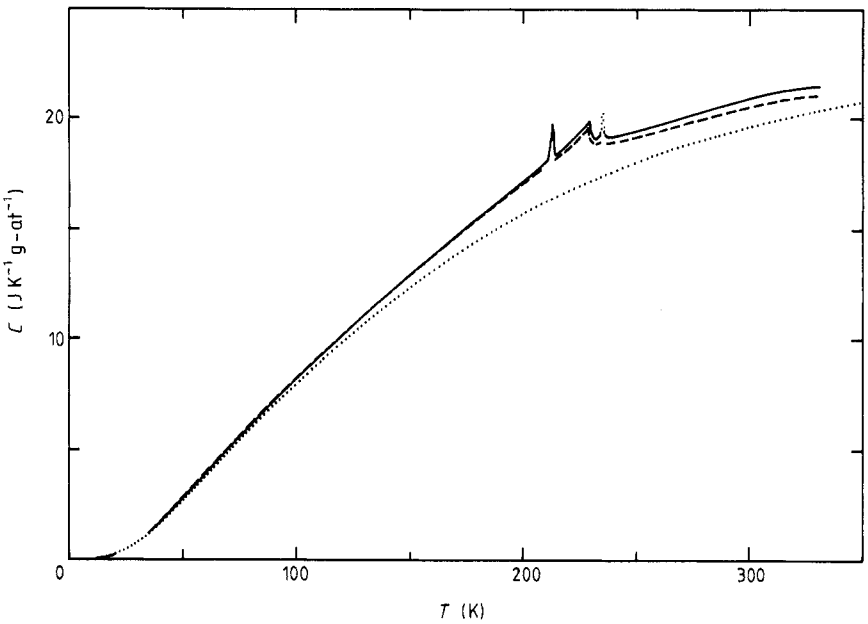

Figure 3. Specific heat of CuO up to room temperature. Full curve, experimental data; broken curve, specific heat at constant volume (corrected for the dilatation term); dotted curve, lattice specific heat according to the measured phonon DOS.

Turning now to high-T_c superconductors, it is possible that at least part of the low-temperature linear terms found in $YBa_2Cu_3O_{7-y}$ [13] has the same origin, especially in view of the sample dependence of both γ^* and β and their correlated variation. This correlation—the higher the γ^*, the lower the θ—follows naturally if the sample-dependent excess calorimetric contribution is attributed to a single T^2 term that depends on porosity and crystallinity. If this explanation is rejected, the large sample-dependent variation of the Debye temperature, which is not reflected in the elastic constants, becomes a puzzle.

4.3. High-temperature specific heat

High-temperature data are presented in figure 3. About 1500 points are included. The data are normalised to one gram-atom (half a mole). An enlargement of the transition region is shown in figure 4. At $T_N = 229.5$ K (midpoint), a step-like anomaly marks the onset of 3D antiferromagnetism. At $T_M = 212.6$ K (top), a peak coincides with the incommensurate–commensurate transition. The present data do not provide a proof of a first-order transition, but we note that the width of the peak is dominated by the instrumental resolution. This is evidenced by a comparison with the first-order peak at 234.7 K, which is extrinsic and due to the melting of 1.0 mg of silicone grease used to attach the sample. The latent heat for the incommensurate–commensurate transformation is 4.5 J mol^{-1} or $0.0025\ RT_M$. This figure is consistent with the result of LMJO, although the anomaly is sharper (doubled height) in the present case.

The effective Debye temperature is shown in figure 5. The calculation is done with partial allowance for anharmonicity, according to

$$C_V = C_p - AC_V^2T$$

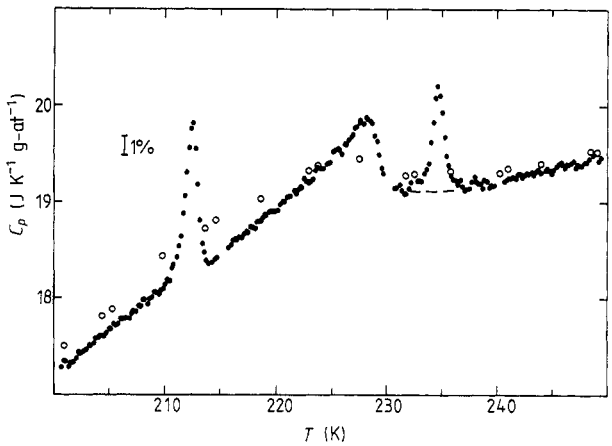

Figure 4. Full circles, specific heat in the vicinity of the magnetic transitions. The peak at 234.5 K is due to the melting of 1.0 mg of silicone grease used to attach the sample. Open circles, data of Hu and Johnston [7].

where $A = 2.7 \times 10^{-6}$ g-at J^{-1} (we use the estimate of LMJO for consistency). This correction represents 1.6% of C_p at 300 K. The result of the computation represents the true Debye temperature inasmuch as the other contributions (mainly magnetic) may be neglected, i.e. far from the critical region. In the present case, the shape of the $\theta(T)$

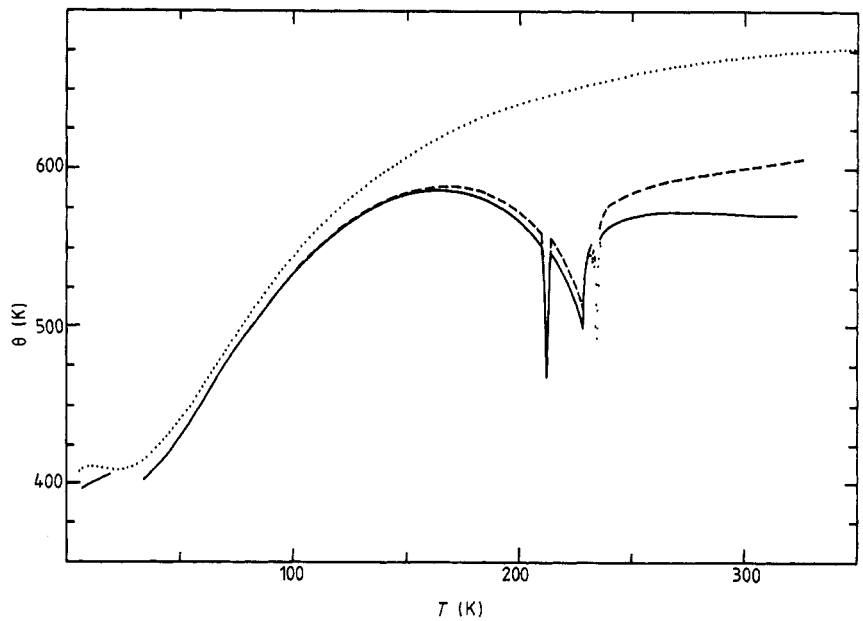

Figure 5. Effective Debye temperature θ versus temperature. Full curve, calculated directly from C_p (without correction for the magnetic contribution); broken curve, θ calculated from C_V; dotted curve, θ calculated from the phonon DOS.

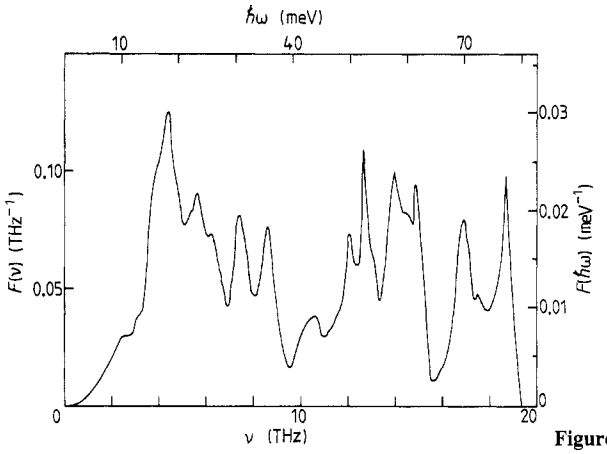

Figure 6. Phonon DOS of CuO.

curve above the magnetic transitions is unphysical, suggesting a significant contribution of magnetic short-range order. This remark was the starting point of LMJO, who constructed an extrapolation of the lattice specific heat to isolate the magnetic contribution. In the present study, we obtain the lattice specific heat from a measurement of the phonon density-of-states.

The specific heat and the phonon spectrum were not measured on the same sample. The sintered sample with its small size and large surface-to-volume ratio favours complete oxidation and homogeneity of the magnetic properties. Neutron scattering on the other hand evidently requires a large single crystal. However, we are confident that the high-temperature (>100 K) lattice specific heat that we extract from the latter experiment is not sample-dependent. An experimental proof of this assertion is given by a comparison of the *total* specific heat of three samples from three laboratories *above* the magnetic transitions. At $T = 250$ K, Hu and Johnson [7] find $C_p = 39.11$ J mol^{-1} K^{-1}, Loram *et al* [12] 39.13 J mol^{-1} K^{-1} and our result (table 1 later) is 38.97 J mol^{-1} K^{-1}. The relative deviations from the mean are +0.11%, +0.14% and −0.25%, respectively. The possible sample dependence of the high-temperature lattice specific heat can therefore not be a significant source of error (see figure 3). The sample dependence of the low-temperature specific heat on the other hand (figure 2) has no effect on the study of the magnetic contribution, as can be seen on figure 3.

4.4. Phonon density of states

The phonon density of states was deduced from measurements of the phonon dispersion curves performed on the triple-axis spectrometer 2T at the Orphée reactor. As there are 8 atoms in the monoclinic unit cell there are 24 phonon branches in each direction of the reciprocal space. More than 60 branches have been measured at room temperature in 6 different directions. The data were used to adjust the parameters of a rigid-ion model from which the phonon DOS and the lattice contribution C_l to the specific heat were calculated. The phonon DOS of CuO is depicted in figure 6. There is no gap in the spectrum but the minimum at 9.5 THz indicates a separation between low-frequency Cu-like modes and high-frequency O vibrations. The high-frequency cutoff (19.3 THz) is considerably higher than in the related transition metal monoxides (MnO: 16.5 THz, FeO: 15 THz, NiO: 17.5 THz) and there is more DOS in the region close to the cut-off. This indicates that the dynamical metal–oxygen forces in CuO are much stronger than

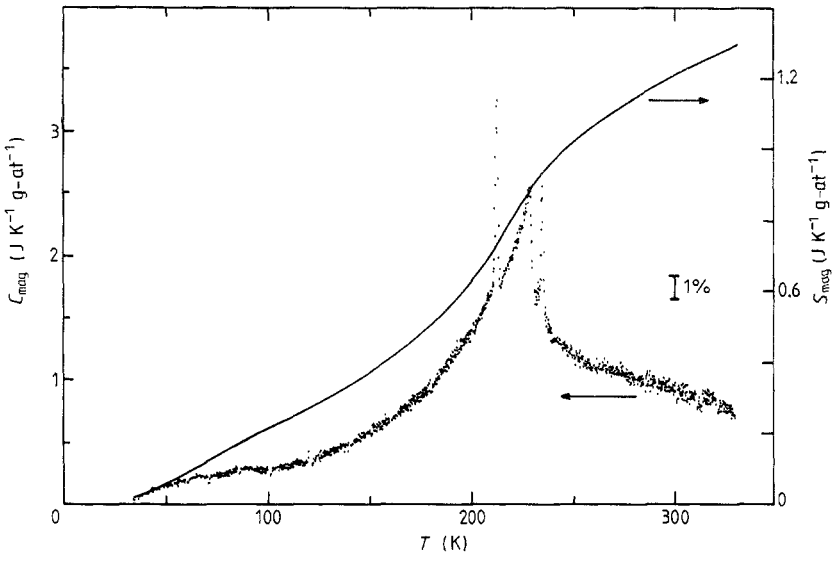

Figure 7. Dots, magnetic specific heat, $C_{mag} = C_V - C_{phonon}$, according to the present measurements; full curve, magnetic entropy, S_{mag}. The expected asymptotic value is 2.88 J K^{-1} g-at^{-1} for $S = \frac{1}{2}$.

in the other monoxides. The calculated temperature dependent Debye temperature $\theta(T)$ (see figure 5) does not show the usual increase at very low temperatures. This can be traced back to an upward curvature of some transverse acoustic branches. The value of $\theta = 404$ K at 4 K (the lowest temperature in the calculation) has to be compared with $\theta(0) = 390 \pm 10$ K as determined from the specific heat measurement. Considering that small errors may be introduced by deficiencies of our lattice dynamical model the agreement is very satisfactory. At higher temperatures the calculated specific heat is much less sensitive to details in the phonon DOS. Therefore, it is expected to be rather accurate. More details about the phonon measurements in CuO will be given in a forthcoming publication [22].

5. Discussion

The magnetic specific heat C_{mag}, obtained by subtraction of the calculated lattice contribution, is shown in figure 7. An interesting test of the consistency of the magnetic and thermal data is given by Fisher's relation for antiferromagnets [23, 24]:

$$\chi \simeq (C/T)(U_m(T) - U_m(0))/(U_m(\infty) - U_m(0)) \tag{1}$$

where U_m is the magnetic energy, χ the magnetic susceptibility and C the Curie constant. The susceptibility was recalculated from the thermal data of figure 7 and scaled using $C/(U_m(\infty) - U_m(0)) = 5.25 \times 10^{-5}$ emu K J^{-1} and an additive constant $\chi_0 = 1.84 \times 10^{-6}$ emu g^{-1} (these parameters were obtained by a fit in the 200–250 K region, where C_{mag} is most accurate). The result is shown in figure 1 as a continuous line. The physical significance of the fitted parameters is limited by the fact that equation (1) is valid for $\chi_\parallel$ while we measure an average of $\chi_\perp$ and $\chi_\parallel$ in a polycrystal; we note however that the overall behaviour is qualitatively reproduced. In particular, the smallness of the cusp in the susceptibility at T_N appears to be consistent with the low energy involved in the long-range ordering process.

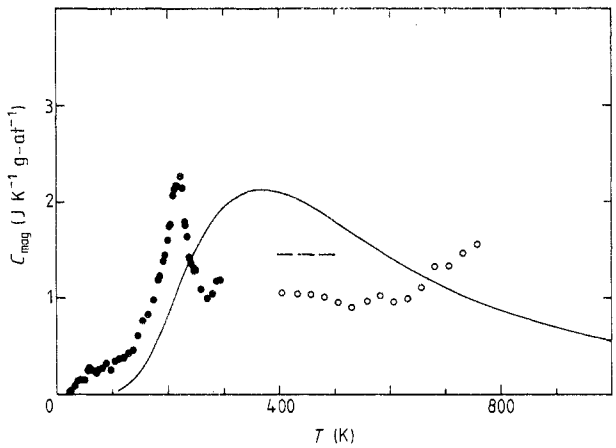

Figure 8. Magnetic specific heat based on the data of Hu and Johnston [7] below 300 K (●), and that of Wöhler and Jochum [25] above 300 K (○). A dilatation correction is applied and the lattice specific heat deduced from the phonon DOS is subtracted. The entropy according to this plot is $\frac{3}{4}R \ln 2$ at 770 K. Full curve, Schottky contribution calculated in the Cu^{2+} cluster model; broken line, maximum specific heat in the 1D and 2D, $S = \frac{1}{2}$ Heisenberg antiferromagnets (see text).

Compared to other 3d transition metal oxides, CuO displays an unusual behaviour in many respects. The susceptibility does not peak at the Néel temperature, but shows a broad maximum at $\simeq 2.35T_N$ [4]. The paramagnetic tail at $T \gg T_N$ is hardly observed at all [4]. The ordered moment below T_N measured by neutron diffraction, $0.65\mu_B$ [2, 11], is substantially smaller than the expected value $g\mu_B S \simeq 1.1\mu_B$. The amplitude of the calorimetric transition at T_N is small, the entropy loss below T_N is only 31% of $R \ln 2$, and the short-range order contribution above T_N is large. These last points are made evident by the plots of $C_{mag} = C_V - C_l$ of figures 7 and 8.

A model of molecular antiferromagnetism was proposed by O'Keefe and Stone [3]. Cu^{2+} ions are assumed to form binuclear complexes, each ion with one unpaired electron. The cupric ions interact to form a singlet ground state ($S = 0$) and a higher triplet ($S = 1$). The susceptibility curve results then from two contributions. Long-range ordering dominates the low-temperature part, and contributes by a rapidly decreasing paramagnetic tail in the intermediate range. The high-temperature part is essentially given by the Schottky contribution of the two-level binuclear system. O'Keefe and Stone [3] obtain a fit in the latter region with $g = 2$ and a level separation $J/k_B = 1050$ K. In figure 8 we show the calculated Schottky specific heat for the proposed model, compare it with the specific heat measurements of Hu and Johnston (15–300 K) [7] and Wöhler and Jochum (400–770 K) [25], after subtracting the lattice specific heat. The proposed model is not supported by thermodynamic data, even if one allows for large uncertainties in measurements and anharmonic corrections.

As pointed out by LMJO, low dimensionality magnetic coupling constitutes an attractive alternative explanation. Antiferromagnetic systems with similar behaviours have been reported in the literature. The closest probably is $Mn(HCOO)_2.2H_2O$, a 2D Heisenberg antiferromagnet with $S = \frac{5}{2}$: its specific heat [26, 27] shows a long-range ordering anomaly at 3.7 K superimposed on a broad hump due to short-range order, and a first-order peak at 1.7 K due to spontaneous reorientation of the antiferromagnetic axis. A number of such systems are reviewed in [18] in the frame of the 1D, 2D and 3D Ising, *XY* and Heisenberg models. The interaction of Cu^{2+} ions is quite generally of

the Heisenberg type, i.e. isotropic. It is well known that ideal 1D and 2D Heisenberg antiferromagnets do not undergo a transition to long-range order at any non-zero temperature. The entropy has to be removed by short-range correlations, and a broad Schottky-like anomaly dominates the magnetic specific heat. However 3D coupling, however small, always exists in real 1D or 2D systems, and at sufficiently low temperatures triggers quite generally a transition to long-range order. As a result, a sharp feature at T_N is superimposed on a broad anomaly in the specific heat. The ratio between T_N and the temperature of the susceptibility maximum can be considered to be a measure of the ratio J'/J, where J' is the out-of-chain (or out-of-plane) coupling, and J is the 1D (or 2D) Heisenberg interaction. In the 3D case, a Néel point is predicted, but the importance of the short-range order contribution above this point is far from negligible and it generally increases when the spin is lowered.

The dimensionality of the antiferromagnetic system is generally not readily determined on the basis of crystallographic data ($KCuF_3$, a cubic perovskite, behaves as a 1D antiferromagnet), but rather is deduced from the application of criteria based on the specific heat and the magnetic susceptibility. Loosely speaking, the lower the dimensionality, the larger the specific heat tail above T_N, the larger the difference between the temperature where the susceptibility is maximum and T_N, and the larger the difference between the maximum susceptibility and the susceptibility at T_N (Ising case).

A first criterion may sometimes be found in the behaviour of the heat capacity at low temperatures. The antiferromagnetic spin wave specific heat behaves as T^d where d is the dimension. We have shown that the low-temperature (<4 K) linear term γ^* is extremely small, and probably not intrinsic. A T^2 contribution is not excluded by polynomial fits, but is not convincingly separated from the lattice contribution. According to this criterion, we would conclude that $d \geqslant 2$, but we note that in some cases (e.g. $CuF_2.2H_2O$, [18]) the presence of 3D ordering at T_N due to J' opens a gap and depresses the low-temperature magnetic specific heat below the spin-wave prediction for $d = 1$ or 2.

Another test for the determination of the dimensionality is the entropy removed below T_N, which literally makes sense only in the 3D case. We find $S_m(229.5\ \text{K}) = 0.31\ R \ln 2$. This is about one-half of the experimental findings for the 3D, spin $\frac{1}{2}$ Heisenberg antiferromagnets $CuCl_2.2H_2O$, NdGaG and SmGaG (G = garnet) [18]. The short-range order contribution in CuO above T_N is clearly larger, and points to lower dimensionality. Another reason for rejecting the 3D case is the difference between the temperature where the magnetic susceptibility is maximum, $T_{max} \simeq 540$ K [3], and the long-range ordering temperature, $T_N = 230$ K. Using the high-temperature series expansion technique [18], the corresponding difference in the 3D Heisenberg antiferromagnet is expected to be of the order of only 20%—and indeed it is found experimentally to be about 15% in the case of $CuCl_2.2H_2O$ [18]. From these comparisons we conclude that $d \leqslant 2$.

Criteria used to discriminate between the 2D and 1D case cannot involve T_N, which appears as a deviation from the ideal case $J' = 0$. One may still use the shape of the susceptibility and specific heat above T_N. LMJO have shown that the high-temperature susceptibility, mainly the broad maximum, can be equally well fitted within the 1D or the 2D models. In the first case, the isotropic interaction and g-factor are $J/k_B = 460$ K and $g = 2.21$, and in the second case $J/k_B = 306$ K and $g = 2.25$ (quadratic lattice). What are the consequences of these models for the specific heat? In the 1D chain model, numerical calculations predict a maximum in the specific heat, $C_{mag}^{max} = 0.350R$ at $T = 0.962\ J/k_B$. Similar calculations are not available for the 2D model, but based on a review of

experimental findings, de Jongh and Miedema [18] predict a maximum specific heat $C_{mag}^{max} \simeq 0.35R$ at $T \simeq 1.4\,J/k_B$ for the 2D Heisenberg antiferromagnet with $S = \frac{1}{2}$. Thus 1D and 2D models yield indistinguishable temperatures (440 and 430 K) and amplitudes ($0.35R$) for the maximum of the specific heat. This predicted maximum is at best compatible with the early high-temperature specific heat data [25] after subtraction of the presently determined lattice specific heat (figure 8). More precise data in this temperature range are clearly needed to confirm the 1D or 2D pictures, but could not discriminate between them.

According to LMJO, the entropy (which may be compared with theoretical predictions only in the short-range order region, i.e. above T_N) favours the 1D interpretation rather than the 2D one. A fair agreement between theory and experiment is found in the 1D case and a 60% difference in the 2D case. Our data for C_{mag}, although obtained in a different way, agree quantitatively with those of LMJO and the same conclusion may be retained. We note, however, that only the 1D Heisenberg has been the subject of full numerical evaluation [28]. In the 2D case, one must rely on spin-wave theory in the low-temperature region ($T \ll T_N/2$) to compute the entropy at T_N. Based on comparisons between experiment, numerical calculations and spin-wave theory, the adequacy of the spin-wave approach to yield correct amplitudes in the $S = \frac{1}{2}$ case has been questioned, however, both for 1D and 2D systems [18]. The entropy argument thus does not appear entirely conclusive.

We conclude that 1D *or* 2D antiferromagnetic order best describes the thermal and magnetic properties of CuO. A verification of the occurrence of the specific heat maximum near 430–440 K is desirable. An extension of numerical calculations to the 2D, $S = \frac{1}{2}$ Heisenberg antiferromagnet appears necessary to discriminate between 1D and 2D order based on thermodynamic data alone. The situation is complicated in the present case by the magnitude of the interaction that causes the long-range ordering ($J'/J \simeq 0.1$ [12]) which makes CuO a rather poor example of a low-dimensional antiferromagnet.

The relevance of the study of the magnetic properties of CuO to the problem of high temperature superconductivity lies in the similarity between the susceptibility curves of CuO and those of $La_{2-x}Sr_xCuO_4$ ('LSCO') [29], $YBa_2Cu_3O_{7-y}$ ('YBCO') [29] and $Bi_2Sr_2CaCu_2O_{8+z}$ ('BSCCO') [30]. In both prototype systems LSCO and YBCO, superconductivity sets in when 3D antiferromagnetic order vanishes (i.e. near $x = 0.04$ in LSCO, and $y = 0.5$ in YBCO) [29, 31]. This does not mean that magnetic correlations disappear: the overall behaviour of the susceptibility curves is so similar to that of CuO that we expect low-dimensional, short-range order to persist even when 3D antiferromagnetism has vanished. These similarities include a broad maximum of χ near 800 K in LSCO and YBCO, a positive slope $d\chi/dT$ at lower temperatures after removal of extrinsic Curie terms and a barely detectable anomaly in χ at the Néel temperature when the compound does order (oxygen-deficient La_2CuO_{4-z} is an exception) [29]. In BSCCO superconducting crystals we find [30] a strongly increasing susceptibility curve ($d\chi/dT > 0$) above T_c that cannot be explained by band models—except if pathological density-of-states curves are considered—but which is quite natural for a low-dimensional antiferromagnet (see e.g. CuO between 100 and 250 K). The ordered $YBa_2Cu_3O_{6.5}$ superconducting phase ($T_c = 53$ K) reported in [32] behaves similarly to BSCCO. These analogies strongly suggest that the nature of the magnetic interactions between Cu^{II} sites in high-T_c superconductors is of short range and low dimensionality, leading to a macroscopically *disordered* magnetic state. This state appears to be a prerequisite for the occurrence of superconductivity. This suggests that the ingredients for high-T_c superconductivity are well decoupled 1D or 2D magnetic structures of CuO, leading to

Table 1. Specific heat at constant pressure $C_p(T)$, entropy $S(T)$ and enthalpy $H(T)$ of CuO at selected temperatures. 1 mole = 2 gram-atom = 79.55 g. The estimated accuracy is 1%.

T (K)	C_p (J mol^{-1} K^{-1})	S (J mol^{-1} K^{-1})	$(H - H(0))/T$ (J mol^{-1} K^{-1})
1.5	2.94×10^{-4}	1.61×10^{-4}	0.98×10^{-4}
4.2	4.96×10^{-3}	1.79×10^{-3}	1.31×10^{-3}
25	0.948	0.315	0.236
50	5.71	2.28	1.68
75	11.31	5.67	3.97
100	16.48	9.65	6.47
125	21.38	13.84	8.97
150	25.99	18.14	11.42
175	30.23	22.44	13.81
200	34.45	26.72	16.13
225	38.90	31.00	18.42
250	38.97	35.02	20.45
275	40.54	38.76	22.20
298.16	41.80	42.03	23.68
300	41.88	42.28	23.79
325	42.93	45.62	25.22

the absence of phase transition in Heisenberg lattices, plus sufficient doping to delocalize charge carriers and provide electrical conductivity. We note that very recent, unpublished theoretical work [33] indeed suggests that the disordered Heisenberg lattice of antiferromagnetic coupled copper spins serves a role analogous to the phonons in a conventional superconducting system.

With this in mind, the standard decomposition of the total susceptibility of the superconducting oxides above T_c into core, van Vleck, Pauli and Landau–Peierls terms may miss an important contribution due to short-range antiferromagnetic correlations (which happens to be nearly constant in restricted temperature ranges). It follows that estimates of the density-of-states at the Fermi level in superconducting oxides based on the absolute value of the total susceptibility alone should be considered with caution.

As a final remark, it is interesting to note how some properties of the high-T_c phases reflect those of their building blocks (assuming that inhomogeneity effects are negligible). Bumps in the resistivity curves near 220 K in the La_2CuO_4 semiconductor [34] may be related to the magnetic transition of the CuO_x structure elements. We also note that in a recent specific heat measurement of a single crystal of YBCO, anomalies are found [35] at 230 and 212 K, again reflecting the properties of pure CuO.

6. Thermodynamic functions

Table 1 gives the heat capacity and derived thermodynamic functions for cupric oxide at selected integral values of temperature. The silicone peak at 234.5 K was removed before integration of C_V/T and C_p. For a discussion the reader is referred to [7].

7. Conclusion

A calorimetric study of the magnetic transitions in CuO was presented. The commensurate–incommensurate transition at 212.6 K was found to be of first order with a

very small anisotropy energy. The antiferromagnetic–paramagnetic transition at 229.5 K has a critical rather than mean-field shape, showing that the spatial range of magnetic interactions is short. Using the lattice specific heat obtained from a measurement of the phonon DOS, we separated the magnetic specific heat. The latter shows an important short-range order contribution. The behaviour of both the specific heat and susceptibility is best described in the frame of the 1D or 2D, $S = \frac{1}{2}$ Heisenberg model, in agreement with the suggestion of LMJO. It is suggested that the magnetic properties of high-T_c superconductors are of the same nature, although complicated by the delocalisation of charge carriers.

A sample dependence of the low-temperature specific heat was observed, and was related to the presence of surface-phonon contributions in incompletely sintered material.

After completion of this work we became aware of recent published and unpublished work. The observation of rounded peaks near 215 and 230 K in specific heat measurements has been reported [36]. In a study of the magnetic neutron scattering of single crystal cupric oxide, antiferromagnetic ordering along the $(10\bar{1})$ chains has been confirmed [37], hysteretic behaviour at T_M has been found and strong correlations above T_N have been observed.

Acknowledgments

The authors are grateful to L Schellenberg for x-ray characterisation. They acknowledge fruitful discussions and two-way data exchange with J W Loram, and particularly thank him for sending an early preprint of his own study of CuO. This work was supported by the Fonds National Suisse de la Recherche Scientifique.

References

[1] Tunnell G, Posnjak E and Ksanda C J 1933 *J. Wash. Acad. Sci.* **23** 195; 1935 *Z. Kristallogr.* **90** 120
[2] Brockhouse B N 1954 *Phys. Rev.* **94** 781
[3] O'Keefe M and Stone F S 1962 *J. Phys. Chem. Solids* **23** 261
[4] Perakis N, Serres A and Karantassis T 1956 *J. Phys. Radium* **17** 134
[5] Parkin S S P, Engler E M, Lee V Y and Beyers R B 1988 *Phys. Rev.* B **37** 131
[6] Paleari A, Parmigiani F, Parravicini G B, Ripamonti N, Samoggia G and Scagliotti M 1988 *Physica* C **153–5** 508
[7] Hu J-H and Johnston H L 1953 *J. Am. Chem. Soc.* **75** 2471. Figure 1 of this article shows that traces of the 212 K anomaly were apparent in the earlier work of Millar R W 1929 *J. Am. Chem. Soc.* **51** 215
[8] Todd S S and Bonnikson K R 1951 *J. Am. Chem. Soc.* **73** 3894
[9] King E G 1957 *J. Am. Chem. Soc.* **79** 2399
[10] King E G and Christensen A U Jr 1958 *J. Am. Chem. Soc.* **80** 1800
[11] Forsyth J B, Brown P J and Wanklyn B M 1988 *J. Phys. C: Solid State Phys.* **21** 2917
[12] Loram J W, Mirza K A, Joyce C P and Osborne A J 1988 *Europhys. Letters* **8** 263
[13] Eckert D, Junod A, Bezinge A, Graf T and Muller J 1988 *J. Low-Temp. Phys.* **73** 241
[14] Åsbrink S and Norrby L-J 1970 *Acta Crystallogr.* B **26** 8
[15] Pelizzone M and Treyvaud A 1981 *Appl. Phys.* **24** 375
[16] Junod A, Bezinge A and Muller J 1988 *Physica* C **152** 50
[17] Martin D L 1987 *Rev. Sci. Instrum.* **58** 639
[18] de Jongh L J and Miedema A R 1974 *Adv. Phys.* **23** 1
[19] Bizette H and Tsai B 1955 *C. R. Acad. Sci., Paris* **241** 183
[20] Golding B, Birge N O, Haemmerle W H, Cava R J and Rietman E 1987 *Phys. Rev.* B **36** 5606

[21] Pohl R O 1981 *Springer Topics in Current Physics* vol. 24, ed. W A Phillips (Berlin: Springer) p 46
[22] Reichardt W, Gompf F, Aïn M and Wanklyn B M to be published
[23] Fisher M E 1962 *Phil. Mag.* **7** 1731
[24] Skalyo J Jr, Cohen A F, Friedberg S A and Griffiths R B 1967 *Phys. Rev.* **164** 705
[25] Wöhler L and Jochum N 1933 *Z. Physik. Chem.* A **167** 169
[26] Pierce R D and Friedberg S A 1968 *Phys. Rev.* **165** 680; 1971 *Phys. Rev.* B **3** 934
[27] Matsuura M, Blöte H W J and Huiskamp W J 1970 *Physica* **50** 444
[28] Bonner J C and Fisher M E 1964 *Phys. Rev.* **135** A640
[29] Johnston D C, Sinha S K, Jacobson A J and Newsam J M 1988 *Physica* C **153–5** 572
[30] Shaltiel D, Bill H, Decroux M, Hagemann H, Junod A, Peter M, Ravi Sekhar Y, Triscone G, Walker E and Zhao Z X 1988 *Physica* C **157** 240
[31] Kumagai K, Watanabe I, Aoki H, Nakamura Y, Kimura T, Nakamichi Y and Nakajima H 1988 *Superconducting Materials* ed. S Nakajima and H Fukuyama (*Japan. J. Appl. Phys.* Series 1) (Tokyo: Japan J. Appl. Phys.) p 37
[32] Takabatake T, Ishikawa M, Nakazawa Y and Koga K 1988 *Preprint*
[33] Guo Y, Langlois J-M and Goddard III W A 1988 *Science* **239** 896
Chen G and Goddard III W A 1988 *Science* **239** 899
[34] Beille J, Chevalier B, Demazeau G, Deslandes F, Etourneau J, Laborde O, Michel C, Lejay P, Provost J, Raveau B, Sulpice A, Tholence J L and Tournier R 1987 *Physica* B **146** 307
[35] Fossheim K, Nes O M, Laegreid T, Darlington C N W, O'Connor D A and Gough C E 1988 *Int. J. Mod. Phys.* B **2** 1171
[36] Seehra M S, Feng Z and Gopalakhrishnan R 1988 *J. Phys. C: Solid State Phys.* **21** L1051
[37] Yang B X, Tranquada J M and Shirane G 1988 *Phys. Rev.* B **38** 174